



BRNO UNIVERSITY OF TECHNOLOGY

VYSOKÉ UČENÍ TECHNICKÉ V BRNĚ

FACULTY OF MECHANICAL ENGINEERING

FAKULTA STROJNÍHO INŽENÝRSTVÍ

INSTITUTE OF MATHEMATICS

ÚSTAV MATEMATIKY

**PARAMETER OPTIMIZATION OF THE MODIFIED PHASE
CORRELATION METHOD FOR SUB-PIXEL IMAGE
REGISTRATION**

OPTIMALIZACE PARAMETRŮ MODIFIKOVANÉ FÁZOVÉ KORELACE PRO SUB-PIXELOVOU REGISTRACI
OBRAZŮ

BACHELOR'S THESIS

BAKALÁŘSKÁ PRÁCE

AUTHOR

AUTOR PRÁCE

Petra Kosová

SUPERVISOR

VEDOUCÍ PRÁCE

Mgr. Jana Hoderová, Ph.D.

BRNO 2016

Zadání bakalářské práce

Ústav: Ústav matematiky
Studentka: **Petra Kosová**
Studijní program: Aplikované vědy v inženýrství
Studijní obor: Matematické inženýrství
Vedoucí práce: **Mgr. Jana Hoderová, Ph.D.**
Akademický rok: 2016/17

Ředitel ústavu Vám v souladu se zákonem č.111/1998 o vysokých školách a se Studijním a zkušebním řádem VUT v Brně určuje následující téma bakalářské práce:

Optimalizace parametrů modifikované fázové korelace pro sub-pixelovou registraci obrazů

Stručná charakteristika problematiky úkolu:

Cílem práce je zjistit optimální parametry frekvenčního filtru použitého ve fázové korelaci pro dosažení maximální přesnosti určení vzájemného posunu dvou digitálních obrazů.

Cíle bakalářské práce:

Nalézt analytický předpis pro optimální frekvenční filtr pro fázovou korelaci.

Seznam literatury:

DRUCKMÜLLEROVÁ, Hana. Phase correlation: the mathematical background and application to image registration. Saarbrücken, Germany: Lambert Academic Publishing, 2011. ISBN 3846550914.

Termín odevzdání bakalářské práce je stanoven časovým plánem akademického roku 2016/17

V Brně, dne

L. S.

prof. RNDr. Josef Šlapal, CSc.
ředitel ústavu

doc. Ing. Jaroslav Katolický, Ph.D.
děkan fakulty

Abstrakt

Práce je zaměřena na určení parametrů váhové funkce, která je pak použita pro určení posunu mezi dvěma obrazy se sub-pixelovou přesností. Jsou použity standartní techniky pro registraci obrazů jako je Fourierova transformace, fázová korelace, bilineární interpolace aj. V práci je zahrnuta potřebná teorie, hledané parametry, postup optimalizace a je přiložen i program, který sloužil jako optimalizační prostředek.

Abstract

The goal of this thesis is to find parameters of weight function, thanks to them we will gain searched shift vector with sub-pixel precision. We are applying Fourier transform, inverse Fourier transform, phase correlation, bilinear interpolation etc. This thesis includes theory, wanted parameters, process of optimization and there is also enclosed program, which helped us with optimization.

klíčová slova

Fourierova transformace, fázová korelace, sub-pixelová přesnost, optimalizace

keywords

Fourier transform, phase correlation, sub-pixel precision, optimization

I declare that I have written the Bachelor's thesis *Parameter optimization of the modified phase correlation method for sub-pixel image registration* on my own and under the guidance of my Bachelor's thesis supervisor Mgr. Jana Hoderová, Ph.D., and using the sources listed in references.

May 5, 2017

Petra Kosová

I would like to thank my supervisor Mgr. Jana Hoderová for her guidance and assistance. I especially thank prof. Miloslav Druckmüller for his big patience and goodwill to explain me how do some specific mathematics methods work.

Petra Kosová

Contents

1	Introduction	12
2	Phase correlation	13
2.1	Basic notions	13
2.2	Fourier transform	14
2.2.1	Implementation	14
2.2.2	Properties of the Fourier transform	15
2.3	Convolution	17
2.4	Various correlation	17
2.4.1	Cross-power spectrum	17
2.4.2	Correlation function	18
3	Image registration	19
3.1	Registration of shifted images	19
3.2	Registration of real images	21
3.2.1	Registration of shifted images step by step	22
3.3	Sub-pixel precision registration	22
3.3.1	Bilinear interpolation	23
4	Program	24
5	Parameter Optimization	26
5.1	Chosen constants and methods	26
5.2	Proper optimization	26
6	Conclusion	29
	Bibliography	31
	Used symbols	33
	Attachment	35

Chapter 1

Introduction

Digital images are everywhere these days. We can find them in many scientific, consumer, industrial and artistic applications. Digital image processing continues to enable the multimedia technology we are experiencing today. Some important examples of image processing include the removal of degradations images suffer during acquisition, compression and transmission of images, economical storage and efficient transmission.

On the Brno University of Technology there is a group of mathematicians who are specialized in processing of different images of the Sun. The leader of this group is prof. Druckmüller from Faculty of Mechanical Engineering.

The Sun is very fascinating object and it's also very important for living on the Earth. If something happened on the Sun it could affect us all, actually it could have deadly impact. Therefore we should study more this interesting star.

Nowadays we know (almost precisely) movements of planets in our solar system. We could estimate the rotational speed of the Sun. However it's still really hard to say something about the motion on the Sun surface. It's a star, so it's a big sphere of gases, which are moving chaotically. Nevertheless sunspots are moving with rotation of the Sun, so their translation is predictable.

Acceptable method for finding out the motion mentioned above is phase correlation, which computes with Fourier transforms and inverse Fourier transforms. This method could compute estimate of shift vector between two images, which refer to translation of the objects in the images. As it was mentioned before, the sun surface is moving chaotically, so the result of phase correlation is not feasible. That's why we divide up the image of the sun to plenty of small segments of size 256×256 and we compute shift vector of all this segment in consequence.

For now we know that the phase correlation is accurate for integer-valued shifts. But the surface motions are so chaotic that we need to improve this method to work with sub-pixel precision. It's done by multiplying the phase correlation function by suitable weight function. In this thesis, we are working with one of small segments and we are looking for proper parameters of weight function.

Chapter 2

Phase correlation

The phase correlation is the motion estimation technique, which is suitable for estimating the global motion of an image, which frame is undergoing. It is also referred to as an image registration approach. The algorithm is rather intuitively clear, and it is based on a simple property of the Fourier transform. The phase correlation is a theme, which could be found in many publications.

Very nice introduction and inspiration to the phase correlation technique could be found in [6]. For our purposes is [1] the optimal choice, where is completely and clearly elaborated theory of registration images.

Therefore in Chapter 2 and 3 is cited [1], unless otherwise specified.

2.1 Basic notions

Definition 2.1. ($\mathcal{L}(\mathbb{R})$) Let us denote $\mathcal{L}(\mathbb{R})$ as the space of all functions $\mathbb{R} \rightarrow \mathbb{C}$ such that

$$\int_{-\infty}^{\infty} |f(x)| dx$$

exists and is finite [2].

Definition 2.2. ($\mathcal{L}(\mathbb{R}^2)$) Let us denote $\mathcal{L}(\mathbb{R}^2)$ as the space of all functions $\mathbb{R}^2 \rightarrow \mathbb{C}$ such that

$$\iint_{\mathbb{R}^2} |f(x, y)| dx dy$$

exists and is finite [2].

Definition 2.3. (Finite function) A function $f(x, y) : \mathbb{R}^2 \rightarrow \mathbb{R}$ is called *finite* if it is equal to zero outside of Cartesian rectangle $\langle a, b \rangle \times \langle c, d \rangle$, where $a, b, c, d \in \mathbb{R}$, $a < b$, $c < d$.

Definition 2.4. (Basic space) Let K be the set of all finite functions φ which have continuous derivatives of all orders. Then $\mathcal{K} = (K, +, \cdot)$ is a vector space called *basic space* with standardly defined operations of functions addition and multiplication by a constant.

Definition 2.5. (Dirac distribution) The *Dirac distribution* is a functional

$$T(\varphi) = \varphi(0, 0)$$

on the basic space \mathcal{K} .

The Dirac distribution is usually written as

$$\iint_{\mathbb{R}^2} \delta(x, y) \varphi(x, y) dx dy,$$

where the symbol $\delta(x, y)$ represents a “function” equal to zero for all $(x, y) \neq (0, 0)$ such

$$\iint_{\mathbb{R}^2} \delta(x, y) dx dy = 1.$$

2.2 Fourier transform

The Fourier transform is very important in engineering, physical sciences and mathematics. It is reversible, linear transform with many important properties. For example in [2] we can find except the theory many applications too. We could say that the Fourier transform breaks a function into an alternate representation, characterized by sines and cosines, which have big usage in modern world of digital electronics.

2.2.1 Implementation

Definition 2.6. (Fourier transform of function in $\mathcal{L}(\mathbb{R}^2)$) Let $f(x, y) \in \mathcal{L}(\mathbb{R}^2)$. The *Fourier transform* of function f is function $\mathcal{F}\{f\}(\xi, \eta) = F(\xi, \eta) : \mathbb{R}^2 \rightarrow \mathbb{C}$ defined as

$$F(\xi, \eta) = \iint_{\mathbb{R}^2} f(x, y) e^{-i(x\xi + y\eta)} dx dy.$$

Function F is also called the *Fourier spectrum* of function f .

Definition 2.7. (Inverse Fourier transform of function in $\mathcal{L}(\mathbb{R}^2)$) Let function $G(\xi, \eta) \in \mathcal{L}(\mathbb{R}^2)$. The *inverse Fourier transform* of function G is function $\mathcal{F}^{-1}\{G\}(x, y) = g(x, y) : \mathbb{R}^2 \rightarrow \mathbb{C}$ defined as

$$g(x, y) = \frac{1}{4\pi^2} \iint_{\mathbb{R}^2} G(\xi, \eta) e^{i(x\xi + y\eta)} d\xi d\eta.$$

Theorem 2.8. (Fourier inversion theorem for function in $\mathcal{L}(\mathbb{R}^2)$) If $f(\xi, \eta), F(\xi, \eta) \in \mathcal{L}(\mathbb{R}^2)$ and f is continuous on \mathbb{R}^2 , then for every $(\xi, \eta) \in \mathbb{R}^2$ it holds

$$\mathcal{F}^{-1}\{\mathcal{F}\{f(x, y)\}\} = \frac{1}{4\pi^2} \iint_{\mathbb{R}^2} F(\xi, \eta) e^{i(x\xi + y\eta)} d\xi d\eta.$$

Definition 2.9. (Amplitude spectrum, phase spectrum) Let function $f(x, y) \in \mathcal{L}(\mathbb{R}^2)$ have Fourier spectrum $F(\xi, \eta)$. The *amplitude spectrum* of function f is a function $A(\xi, \eta) : \mathbb{R}^2 \rightarrow \mathbb{R}_0^+$ defined as

$$A(\xi, \eta) = |\mathcal{F}\{f(x, y)\}| = |F(\xi, \eta)|.$$

The *phase spectrum* of function f is a function $\Phi(\xi, \eta) : \mathbb{R}^2 \rightarrow \langle 0, 2\pi \rangle$ defined as

$$\begin{aligned}\Re F(\xi, \eta) &= A(\xi, \eta) \cos \Phi(\xi, \eta), \\ \Im F(\xi, \eta) &= A(\xi, \eta) \sin \Phi(\xi, \eta).\end{aligned}$$

If $A(\xi, \eta) = 0$ for some (ξ, η) we define $\Phi(\xi, \eta) = 0$.

2.2.2 Properties of the Fourier transform

The basic properties are written up in Table 2.1. List of functions is situated on the left and their Fourier transforms are in the middle. Some of them are shown below. Functions $f(x, y), g(x, y) \in \mathcal{L}(\mathbb{R}^2)$. Further $\alpha, \beta, x_0, y_0, \xi_0, \eta_0$ are real constants.

	function	Fourier transform	name
1	$\alpha f(x, y) + \beta g(x, y)$	$\alpha F(\xi, \eta) + \beta G(\xi, \eta)$	linearity
2	$f(x - x_0, y - y_0)$	$F(\xi, \eta) e^{-i(\xi x_0 + \eta y_0)}$	shift theorem
3	$e^{i(\xi_0 x + \eta_0 y)} f(x, y)$	$F(\xi - \xi_0, \eta - \eta_0)$	modulation theorem
4	$f(\alpha x, \alpha y)$	$\frac{1}{\alpha^2} F\left(\frac{\xi}{\alpha}, \frac{\eta}{\alpha}\right)$	scale-change theorem
5	$f^*(x, y)$	$F^*(-\xi, -\eta)$	complex conjugate
6	$(f * g)(x, y)$	$F(\xi, \eta)G(\xi, \eta)$	convolution

Table 2.1: Properties of the Fourier transform

Theorem 2.10. (Shift theorem) Let $f_1(x, y) \in \mathcal{L}(\mathbb{R}^2)$ and let $F_1(\xi, \eta)$ be its Fourier spectrum. Let us suppose function

$$f_2(x, y) = f_1(x - x_0, y - y_0),$$

where $x_0, y_0 \in \mathbb{R}$ are given constants. Furthermore let us denote $F_2(\xi, \eta)$ as Fourier spectrum of function $f_2(x, y)$. Then it holds

$$\begin{aligned}F_2(\xi, \eta) &= F_1(\xi, \eta) e^{-i(\xi x_0 + \eta y_0)}, \\ A_2(\xi, \eta) &= A_1(\xi, \eta), \\ \Phi_2(\xi, \eta) &= \Phi_1(\xi, \eta) \oplus (-\xi x_0 - \eta y_0),\end{aligned}$$

where \oplus means addition modulo 2π .

Theorem 2.11. (Scale-change theorem) Let $f_1(x, y) \in \mathcal{L}(\mathbb{R}^2)$ and let $F_1(\xi, \eta)$ be its Fourier spectrum. Let us suppose function

$$f_2(x, y) = f_1(\alpha x, \alpha y),$$

where $\alpha \in \mathbb{R}^+$ is a given constant. Let $F_2(\xi, \eta)$ be its Fourier spectrum. Then it holds

$$\begin{aligned} F_2(\xi, \eta) &= \frac{1}{\alpha^2} F_1\left(\frac{\xi}{\alpha}, \frac{\eta}{\alpha}\right), \\ A_2(\xi, \eta) &= \frac{1}{\alpha^2} A_1\left(\frac{\xi}{\alpha}, \frac{\eta}{\alpha}\right), \\ \Phi_2(\xi, \eta) &= \Phi_1\left(\frac{\xi}{\alpha}, \frac{\eta}{\alpha}\right). \end{aligned}$$

Theorem 2.12. (Rotation theorem) Let $f_1(x, y) \in \mathcal{L}(\mathbb{R}^2)$ and let $F_1(\xi, \eta)$ be its Fourier spectrum. Let us suppose function

$$f_2(x, y) = f_1(x \cos \theta - y \sin \theta, x \sin \theta + y \cos \theta),$$

where $\theta \in \langle 0, 2\pi \rangle$ is a given constant. Let $F_2(\xi, \eta)$ be its Fourier spectrum. Then it holds

$$\begin{aligned} F_2(\xi, \eta) &= F_1(\xi \cos \theta - \eta \sin \theta, \xi \sin \theta + \eta \cos \theta), \\ A_2(\xi, \eta) &= A_1(\xi \cos \theta - \eta \sin \theta, \xi \sin \theta + \eta \cos \theta), \\ \Phi_2(\xi, \eta) &= \Phi_1(\xi \cos \theta - \eta \sin \theta, \xi \sin \theta + \eta \cos \theta). \end{aligned}$$

Theorem 2.13. (Similarity theorem) Let $f_1(x, y) \in \mathcal{L}(\mathbb{R}^2)$ and let $F_1(\xi, \eta)$ be its Fourier spectrum. Let us suppose function

$$f_2(x, y) = f_1(\alpha x \cos \theta - \alpha y \sin \theta - x_0, \alpha x \sin \theta + \alpha y \cos \theta - y_0),$$

where $\theta \in \langle 0, 2\pi \rangle, \alpha \in \mathbb{R}^+, x_0, y_0 \in \mathbb{R}$ are given constants. Let $F_2(\xi, \eta)$ be its Fourier spectrum. Then it holds

$$\begin{aligned} F_2(\xi, \eta) &= \frac{1}{\alpha^2} e^{-i(\xi x_0 + \eta y_0)} F_1\left(\frac{\xi}{\alpha} \cos \theta - \frac{\eta}{\alpha} \sin \theta, \frac{\xi}{\alpha} \sin \theta + \frac{\eta}{\alpha} \cos \theta\right), \\ A_2(\xi, \eta) &= \frac{1}{\alpha^2} A_1\left(\frac{\xi}{\alpha} \cos \theta - \frac{\eta}{\alpha} \sin \theta, \frac{\xi}{\alpha} \sin \theta + \frac{\eta}{\alpha} \cos \theta\right), \\ \Phi_2(\xi, \eta) &= \Phi_1\left(\frac{\xi}{\alpha} \cos \theta - \frac{\eta}{\alpha} \sin \theta, \frac{\xi}{\alpha} \sin \theta + \frac{\eta}{\alpha} \cos \theta\right) \oplus (-\xi x_0 - \eta y_0). \end{aligned}$$

Theorem 2.14. Let $f(x, y) \in \mathcal{L}(\mathbb{R}^2)$ and let $F(\xi, \eta)$ be its Fourier spectrum. The Fourier spectrum of the complex conjugate of function f is the complex conjugate of its Fourier spectrum with reversed axes

$$\mathcal{F}\{f^*(x, y)\} = F^*(-\xi, -\eta).$$

Moreover if f is continuous, then the inverse Fourier transform of the complex conjugate of spectrum F is the complex conjugate of function f with reversed axes

$$\mathcal{F}^{-1}\{F^*(\xi, \eta)\} = f^*(-x, -y).$$

2.3 Convolution

Definition 2.15. (Convolution) Let functions $f_1(x, y), f_2(x, y) \in \mathcal{L}(\mathbb{R}^2)$. The *convolution* $f_1 * f_2$ of functions f_1, f_2 is a function

$$f(x, y) = \iint_{\mathbb{R}^2} f_1(s, t) f_2(x - s, y - t) ds dt.$$

Theorem 2.16. Let functions $f_1(x, y), f_2(x, y) \in \mathcal{L}(\mathbb{R}^2)$ with Fourier spectra $F_1(\xi, \eta), F_2(\xi, \eta)$. Then it holds

$$\mathcal{F}\{f_1(x, y) * f_2(x, y)\} = F_1(\xi, \eta) \cdot F_2(\xi, \eta).$$

Remark 2.17. Proof of Theorem 2.16 could be find in [3].

The fastest way how to compute convolution of f_1 and f_2 is to take the Fourier transform of the first function f_1 and the Fourier transform of the second function f_2 , multiply them and then calculate the inverse Fourier transform of that result. We will see that a very closely related operation is cross correlation function.

2.4 Various correlation

Correlation is used to assess how similar are two different functions.

2.4.1 Cross-power spectrum

Definition 2.18. (Cross-power spectrum) Let functions $f_1(x, y), f_2(x, y) \in \mathcal{L}(\mathbb{R}^2)$ have Fourier spectra $F_1(\xi, \eta), F_2(\xi, \eta)$. The *cross-power spectrum* of function f_1, f_2 is a function $C_{f_1, f_2}(\xi, \eta) : \mathbb{R}^2 \rightarrow \mathbb{C}$ defined as

$$C_{f_1, f_2}(\xi, \eta) = F_1(\xi, \eta) \cdot F_2^*(\xi, \eta).$$

Definition 2.19. (Normalized cross-power spectrum) Let functions $f_1(x, y), f_2(x, y) \in \mathcal{L}(\mathbb{R}^2)$ have Fourier spectra $F_1(\xi, \eta), F_2(\xi, \eta)$. The *normalized cross-power spectrum* of function f_1, f_2 is a function $Z_{f_1, f_2}(\xi, \eta) : \mathbb{R}^2 \rightarrow \mathbb{C}$ defined as

$$Z_{f_1, f_2}(\xi, \eta) = \frac{F_1(\xi, \eta) \cdot F_2^*(\xi, \eta)}{|F_1(\xi, \eta) \cdot F_2(\xi, \eta)|}.$$

Definition 2.20. (Semi-normalized cross-power spectrum) Let functions $f_1(x, y), f_2(x, y) \in \mathcal{L}(\mathbb{R}^2)$ have Fourier spectra $F_1(\xi, \eta), F_2(\xi, \eta)$. The *semi-normalized cross-power spectrum* of function f_1, f_2 is a function $Z_{f_1, f_2}^{p, q}(\xi, \eta) : \mathbb{R}^2 \rightarrow \mathbb{C}$ defined as

$$Z_{f_1, f_2}^{p, q}(\xi, \eta) = \frac{F_1(\xi, \eta) \cdot F_2^*(\xi, \eta)}{(|F_1(\xi, \eta)| + p) \cdot (|F_2(\xi, \eta)| + q)},$$

where $p, q \in \mathbb{R}^+$ are given constants.

2.4.2 Correlation function

Definition 2.21. (Cross-correlation function) Let functions $f_1(x, y), f_2(x, y) \in \mathcal{L}(\mathbb{R}^2)$ have Fourier spectra $F_1(\xi, \eta), F_2(\xi, \eta)$. Function $Q_{f_1, f_2}(x, y) : \mathbb{R}^2 \rightarrow \mathbb{C}$ defined as

$$Q_{f_1, f_2}(x, y) = \mathcal{F}^{-1}\{C_{f_1, f_2}(\xi, \eta)\} = \mathcal{F}^{-1}\{F_1(\xi, \eta) \cdot F_2^*(\xi, \eta)\}$$

is called the *cross-correlation function* of functions f_1, f_2 .

Definition 2.22. (Phase-correlation function) Let functions $f_1(x, y), f_2(x, y) \in \mathcal{L}(\mathbb{R}^2)$ have Fourier spectra $F_1(\xi, \eta), F_2(\xi, \eta)$. Function $P_{f_1, f_2}(x, y) : \mathbb{R}^2 \rightarrow \mathbb{C}$ defined as

$$P_{f_1, f_2}(x, y) = \mathcal{F}^{-1}\{Z_{f_1, f_2}(\xi, \eta)\} = \mathcal{F}^{-1}\left\{\frac{F_1(\xi, \eta) \cdot F_2^*(\xi, \eta)}{|F_1(\xi, \eta) \cdot F_2(\xi, \eta)|}\right\}$$

is called the *phase-correlation function* of functions f_1, f_2 .

Definition 2.23. (Semi-phase correlation function) Let functions $f_1(x, y), f_2(x, y) \in \mathcal{L}(\mathbb{R}^2)$ have Fourier spectra $F_1(\xi, \eta), F_2(\xi, \eta)$. Function $P_{f_1, f_2}^{p, q}(x, y) : \mathbb{R}^2 \rightarrow \mathbb{C}$ defined as

$$P_{f_1, f_2}^{p, q}(x, y) = \mathcal{F}^{-1}\{Z_{f_1, f_2}^{p, q}(\xi, \eta)\} = \mathcal{F}^{-1}\left\{\frac{F_1(\xi, \eta) \cdot F_2^*(\xi, \eta)}{(|F_1(\xi, \eta)| + p) \cdot (|F_2(\xi, \eta)| + q)}\right\}$$

is called the *semi-phase correlation function* of functions f_1, f_2 .

Remark 2.24. Let functions $f_1(x, y), f_2(x, y) \in \mathcal{L}(\mathbb{R}^2)$ be continuous real, i.e. $f_1^* = f_1$ and $f_2^* = f_2$ and with Fourier spectra $F_1(\xi, \eta), F_2(\xi, \eta) \in \mathcal{L}(\mathbb{R}^2)$. Then we can compute the cross-correlation function of f_1 and f_2 as

$$Q_{f_1, f_2}(x, y) = \mathcal{F}^{-1}\{F_1(\xi, \eta) \cdot F_2^*(\xi, \eta)\} = \mathcal{F}^{-1}\{\mathcal{F}\{f_1(x, y)\} \cdot \mathcal{F}\{f_2^*(-x, -y)\}\} = f_1(x, y) * f_2^*(-x, -y) = f_1(x, y) * f_2(-x, -y).$$

Theorem 2.25. (Phase-correlation function of shifted functions) Let function $f_1(x, y) \in \mathcal{L}(\mathbb{R}^2)$ and let $F_1(\xi, \eta)$ be its Fourier spectrum. Let us suppose function $f_2(x, y) = f_1(x - x_0, y - y_0)$, where x_0, y_0 are given constants. Let $F_2(\xi, \eta)$ be the Fourier spectrum of function f_2 . Then the phase-correlation function of functions f_1, f_2 is the Dirac distribution shifted by $(-x_0, -y_0)$

$$P_{f_1, f_2}(x, y) = \delta(x + x_0, y + y_0).$$

Remark 2.26. In whole Chapter 2 we consider function $f(x, y)$ to be defined as $f : \mathbb{R}^2 \rightarrow \mathbb{C}$. When we need to take an image to the frequency domain we change its domain to a bounded area $\{0, 1, \dots, N - 1\} \times \{0, 1, \dots, N - 1\}$, $N \in \mathbb{N}$. Therefore we have to compute with discrete version of Fourier transform or inverse Fourier transform defined as

$$\begin{aligned} \mathcal{D}\{f\}(\xi, \eta) = F(\xi, \eta) &= \sum_{x=0}^{N-1} \sum_{y=0}^{N-1} f(x, y) e^{-\frac{2\pi i}{N}(x\xi + y\eta)}, \\ \mathcal{D}^{-1}\{F\}(x, y) &= \frac{1}{N^2} \sum_{\xi=0}^{N-1} \sum_{\eta=0}^{N-1} F(\xi, \eta) e^{\frac{2\pi i}{N}(x\xi + y\eta)}. \end{aligned}$$

The properties of Fourier transform, just as convolution and correlation stay unmodified, we only swap \mathcal{F} and \mathcal{D} in equations.

Chapter 3

Image registration

Image registration is the process of spatially aligning two images of a scene so that corresponding points assume the same coordinates. The first image will be referred to as the master image and the second as the slave image. For more information see [4].

Definition 3.1. (Digital grey-scale image) Let $R = \{0, 1, \dots, M-1\} \times \{0, 1, \dots, N-1\}$, $M, N \in \mathbb{N}$ and let $W = \{0, 1, \dots, w-1\}$, $w \in \mathbb{N}$. Function

$$f(x, y) : R \rightarrow W$$

is called a *digital grey-scale image* or *image* only if no confusion may be caused. M is called the *image width*, N the *image height*. Elements of R are called *pixels*, value of f in pixel (x, y) is called the *pixel value*. The value of w determines the image *dynamic range*. We say that the *dynamic range is n bits per pixel* or it is an *n -bit image* if $w = 2^n$.

Remark 3.2. We work only with grey-scale image, because in this case it is not important to register colour components of the images.

3.1 Registration of shifted images

We consider that both images thus functions f_1, f_2 are identical but shifted with respect to each other by vector (x_0, y_0) , so

$$f_2(x, y) = f_1(x - x_0, y - y_0).$$

We find out the shift vector by using phase-correlation function. In simple cases we should get discrete impulse function (discrete Dirac impulse), in this case there is one global maximum in coordinates (x_0, y_0) for which we are looking for. If we use original images the result could be ambiguous, due to edges of the images where are the big differences in pixels values. Therefore, it is necessary to cut off or at least smoothen these edges from the images for good shift estimation.

It is achieved by multiplying our image by suitable function g called *window function*. This function must be equal to zero or almost zero at the image edges and continuously tends to one for the rest of the image.

There are number of different window functions which can be used for digital signal processing, like the triangular window, Kaiser window and so on. We will use Gaussian and Hanning window function.

Definition 3.3. (Window function) Let us set

$$\begin{aligned} A &= \langle -a, a \rangle \times \langle -b, b \rangle, & a, b \in \mathbb{R}_0^+, \\ B &= \{(x, y); x^2 + y^2 \leq r^2\}, & r \in \mathbb{R}_0^+. \end{aligned}$$

Let $\sigma \in \mathbb{R}_0^+$ be a given number. Let $\varrho(X, A)$ be the distance of point $X = (x, y)$ from set A , i.e.

$$\varrho(X, A) = \inf \{d \in \mathbb{R}, d = \varrho(X, Y), Y \in A\},$$

where $\varrho(X, Y)$ is the Euclidean metric. Then

1. Function

$$g_{GR}(x, y) = e^{-\frac{\varrho^2(X, A)}{\sigma^2}}$$

is called the *rectangular Gaussian window function*.

2. Function

$$g_{GC}(x, y) = e^{-\frac{\varrho^2(X, B)}{\sigma^2}}$$

is called the *circular Gaussian window function*.

3. Function

$$g_{HR}(x, y) = \begin{cases} \frac{1}{2} + \frac{1}{2} \sin\left(\frac{\pi\varrho(X, A)}{\sigma} - \frac{\pi}{2}\right) & \text{if } \varrho(X, A) \leq \sigma, \\ 0 & \text{if } \varrho(X, A) > \sigma \end{cases}$$

is called the *rectangular Hanning window function*.

4. Function

$$g_{HC}(x, y) = \begin{cases} \frac{1}{2} + \frac{1}{2} \sin\left(\frac{\pi\varrho(X, B)}{\sigma} - \frac{\pi}{2}\right) & \text{if } \varrho(X, B) \leq \sigma, \\ 0 & \text{if } \varrho(X, B) > \sigma \end{cases}$$

is called the *circular Hanning window function*.

Remark 3.4. The window functions are defined as a symmetrical functions with centre in $(0, 0)$ so we have to shift our images by $(\frac{N}{2}, \frac{N}{2})$, it means that we multiply image f by shifted window function $g(x - \frac{N}{2}, y - \frac{N}{2})$.

The advantage of rectangular window functions is that they retain a big part of the image without change. However their drawback is the fact that they do not diminish totally on the edges, it means that there are still some information left. By using circular window function, we miss out on big part of the image, on the other hand we lose the information on the edges. It's possible to use different window functions on both registered images.

Definition 3.5. (Centering images) Let us assume that images f_1, f_2 have width m and height n . Let $N \in \mathbb{N}$ be a number divisible by higher power of 2 (at least 16), not divisible by a high prime number, such that $m \leq N, n \leq N$. Then we create images f_{c1}, f_{c2} from images f_1, f_2 by

$$f_{ck}(x, y) = \begin{cases} f_k(x - m_0, y - n_0) & \text{if } m_0 \leq x \leq m_0 + m - 1, n_0 \leq y \leq n_0 + n - 1, \\ 0 & \text{else} \end{cases}$$

for $k = 1, 2$, where $m_0 = \lfloor \frac{N-m}{2} \rfloor, n_0 = \lfloor \frac{N-n}{2} \rfloor$.

3.2 Registration of real images

Up to this point we have assumed images f_1, f_2 to be identical except for some transformation. Now we use the real images, which may contain additive noise, impulse noise, defects caused by our optical system, dust particles, diffuse light etc.

The cross-correlation function does not need to have clear global maximum, it is why we use semi-phase correlation instead. It could happened that the division by zero occur so we choose p, q to eliminate it. For sharp images we may select small values of p, q , for images which are blurred, taken with poor optics, or at bad conditions, we should increase p, q to decrease influence of frequencies with no information.

Additive noise and variable impulse noise represent information of all spatial frequencies, primary of the highest one. It makes them useless for our registration. Furthermore the low frequencies contain information about optics vignetting and diffuse light of the images. Due to the facts written above, we multiply the Fourier spectra of the image by a suitable weight function to reduce information on the highest/lowest spatial frequencies.

Definition 3.6. (Gaussian low-pass high-pass weight function) Let $\lambda_1, \lambda_2 \in \mathbb{R}_0^+$ and $N \in \mathbb{N}$ be the size of domain of image f . Function $H_{\lambda_1}(\xi, \eta) : \mathbb{R}^2 \rightarrow (0, 1)$ defined as

$$H_{\lambda_1}(\xi, \eta) = e^{-\lambda_1 \frac{\xi^2 + \eta^2}{N^2}}$$

is called the *Gaussian low-pass weight function* with parameter λ_1 . Function $H^{\lambda_2}(\xi, \eta) : \mathbb{R}^2 \rightarrow (0, 1)$ defined as

$$H^{\lambda_2}(\xi, \eta) = 1 - e^{-\lambda_2 \frac{\xi^2 + \eta^2}{N^2}}$$

is called the *Gaussian high-pass weight function* with parameter λ_2 . Function $H_{\lambda_1}^{\lambda_2}(\xi, \eta) : \mathbb{R}^2 \rightarrow (0, 1)$ defined as

$$H_{\lambda_1}^{\lambda_2}(\xi, \eta) = H^{\lambda_2}(\xi, \eta) \cdot H_{\lambda_1}(\xi, \eta)$$

is called the *Gaussian low-pass high-pass weight function*.

Remark 3.7. The weight functions are defined symmetrically with centre in $(0,0)$. We have to shift the images by vector $(\frac{N}{2}, \frac{N}{2})$, i.e. multiply the Fourier spectra of the images by function $H_{\lambda_1}^{\lambda_2}(\xi - \frac{N}{2}, \eta - \frac{N}{2})$.

It's possible to apply Gaussian low-pass high-pass weight function after computing (inverse) Fourier spectra of images, due to the fact that the Gaussian function stay invariable. This weight function is not applicable if there's indispensable amount of additive and variable impulse noise. Therefore we use another type of weight function so called low-pass high-pass weight function.

Definition 3.8. (Low-pass high-pass weight function). Let $r_1, r_2, \sigma_1, \sigma_2 \in \mathbb{R}^+$ such that $r_1 < r_2$. Function $H_{r_1, \sigma_1}(\xi, \eta) : \mathbb{R}^2 \rightarrow (0, 1)$ defined as

$$H_{r_1, \sigma_1}(\xi, \eta) = \begin{cases} 0 & \text{if } \frac{4}{N^2}(\xi^2 + \eta^2) < (r_1 - \sigma_1)^2, \\ \frac{1}{2} + \frac{1}{2} \cos \frac{\pi(r_1 - \frac{2}{N} \sqrt{\xi^2 + \eta^2})}{\sigma_1} & \text{if } (r_1 - \sigma_1)^2 \leq \frac{4}{N^2}(\xi^2 + \eta^2) < r_1^2, \\ 1 & \text{else} \end{cases}$$

is called the *high-pass weight function*. Function $H^{r_2, \sigma_2}(\xi, \eta) : \mathbb{R}^2 \rightarrow (0, 1)$ defined as

$$H^{r_2, \sigma_2}(\xi, \eta) = \begin{cases} 1 & \text{if } \frac{4}{N^2}(\xi^2 + \eta^2) < r_2^2, \\ \frac{1}{2} + \frac{1}{2} \cos \frac{\pi(r_2 - \frac{2}{N} \sqrt{\xi^2 + \eta^2})}{\sigma_2} & \text{if } r_2^2 \leq \frac{4}{N^2}(\xi^2 + \eta^2) < (r_2 + \sigma_2)^2, \\ 0 & \text{else} \end{cases}$$

is called the *low-pass weight function*. Function $H_{r_1, \sigma_1}^{r_2, \sigma_2}(\xi, \eta) : \mathbb{R}^2 \rightarrow \langle 0, 1 \rangle$ defined as

$$H_{r_1, \sigma_1}^{r_2, \sigma_2}(\xi, \eta) = H^{r_2, \sigma_2}(\xi, \eta) \cdot H_{r_1, \sigma_1}(\xi, \eta)$$

is called the *low-pass high-pass weight function*.

3.2.1 Registration of shifted images step by step

Let us denote f_1, f_2 the registered images. The Fourier transform will be computed on a square $N \times N$, where N is even. Steps of registration:

1. Multiplying images f_1, f_2 by window functions. It gives images f_{w1}, f_{w2} .
2. Centering images f_{w1}, f_{w2} in the square $N \times N$ pixels. It gives images f_{c1}, f_{c2} .
3. Computing the semi-normalized cross-power spectrum $Z = Z_{f_{c1}, f_{c2}}^{p, q}$ of images f_{c1}, f_{c2} . Constants p, q are chosen with respect to used optical system, fuzziness, haze etc.
4. Multiplying Z by a low-pass high-pass weight function. It gives Z_w .
5. Computing the inverse discrete Fourier transform P of Z_w .
6. Finding the coordinates of the global maximum of function P , i.e. finding the shift vector (x_0, y_0) .

3.3 Sub-pixel precision registration

The vector (x_0, y_0) is integer valued estimate of the shift vector between images f_1, f_2 . We are looking for sub-pixel precision estimate of the shift vector denoted by $(\tilde{x}_0, \tilde{y}_0)$. There are many methods how to estimate noninteger valued shifts. We will use method based on geometric moments computed from pixel values.

Definition 3.9. (Geometric moment) Let us have circle with centre (x_0, y_0) and radius $\varepsilon \in \mathbb{R}^+$. Then the *geometric moment* is defined as

$$M_{k,l} = \sum_{x^2+y^2 < \varepsilon} \sum x^k y^l P(x_0 + x, y_0 + y), \quad k, l = 0, 1,$$

where $P(x, y)$ is the modified semi-phase correlation function described in step 5 of Subsection 3.2.1 and $M_{0,0}$ is equal to total image intensity (see [4]).

The sub-pixel precision estimate of the shift vector, i.e. the vector $(\tilde{x}_0, \tilde{y}_0)$, is computed as

$$(\tilde{x}_0, \tilde{y}_0) = \left(\frac{M_{1,0}}{M_{0,0}}, \frac{M_{0,1}}{M_{0,0}} \right)$$

and we can consider the point $[\tilde{x}_0, \tilde{y}_0]$ as the centre of gravity of the peak and its neighbourhood with radius ε

Remark 3.10. The sub-pixel precision estimate of the shift vector may be computed also by *bilinear interpolation*. We will use this procedure only for making our own sub-pixel shifts, due to the fact that it is much more faster. On the other hand it's not so accurate.

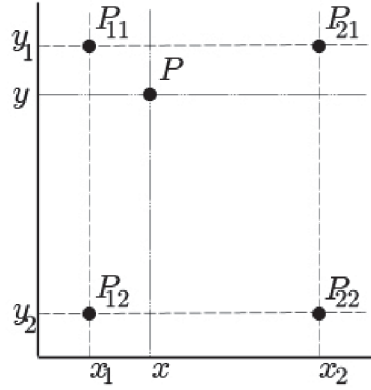


Figure 3.1: Example of 2D grid for bilinear interpolation

3.3.1 Bilinear interpolation

Bilinear interpolation is an extension of linear interpolation for interpolating functions of two variables on a 2D grid. In image processing it's basic resampling technique. It's used for finding out a pixel value of a point in sub-pixel position. We could say, that bilinear interpolation is weighted average in image processing.

Definition 3.11. Let us have points $P_{11} = (x_1, y_1)$, $P_{12} = (x_1, y_2)$, $P_{21} = (x_2, y_1)$, $P_{22} = (x_2, y_2)$ (see Figure 3.1) and assume that we know the pixel value of f in these points . Then it holds

$$\begin{aligned}
 f(x, y_1) &\approx \frac{x_2 - x}{x_2 - x_1} f(P_{11}) + \frac{x - x_1}{x_2 - x_1} f(P_{21}), \\
 f(x, y_2) &\approx \frac{x_2 - x}{x_2 - x_1} f(P_{12}) + \frac{x - x_1}{x_2 - x_1} f(P_{22}), \\
 f(x, y) &\approx \frac{y_2 - y}{y_2 - y_1} f(x, y_1) + \frac{y - y_1}{y_2 - y_1} f(x, y_2).
 \end{aligned}$$

Chapter 4

Program

We would like to find the best parameters for registration of images by the method described before. We used the set of 10 000 images with known sub-pixel shift, for our purpose it was really necessary to make a special program for finding the best parameters. This program is based on procedures developed by Prof. Miloslav Druckmüller and was made under his supervision and the set of testing images was generated by another program created by my colleague Eliška Málková. The program was made in Delphi XE6 and the basic Pascal commands could be found in [5].

In the program presented in this thesis are done some interesting innovations. One of them is remake of the Druckmüller's procedure called **LowPass**, which compute Gaussian low-pass weight function shifted by $\frac{N}{2}$ ($H_{\lambda_1}(\xi - \frac{N}{2}, \eta - \frac{N}{2})$) to procedure called **LowPassHighPass**, which compute shifted Gaussian low-pass high-pass weight function $H_{\lambda_1}^{\lambda_2}(\xi - \frac{N}{2}, \eta - \frac{N}{2})$ defined by Definition 3.6. with respect to Remark 3.7. This new procedure **LowPassHighPass** has four parameters. *Oldspec* referring to cross-power spectrum, *Newspec* computed by this procedure, λ_1 and λ_2 . Further we had to add one parameter called *HPF* (high-pass filter) to procedures **GetTranslation** and **FindImgTranslation**.

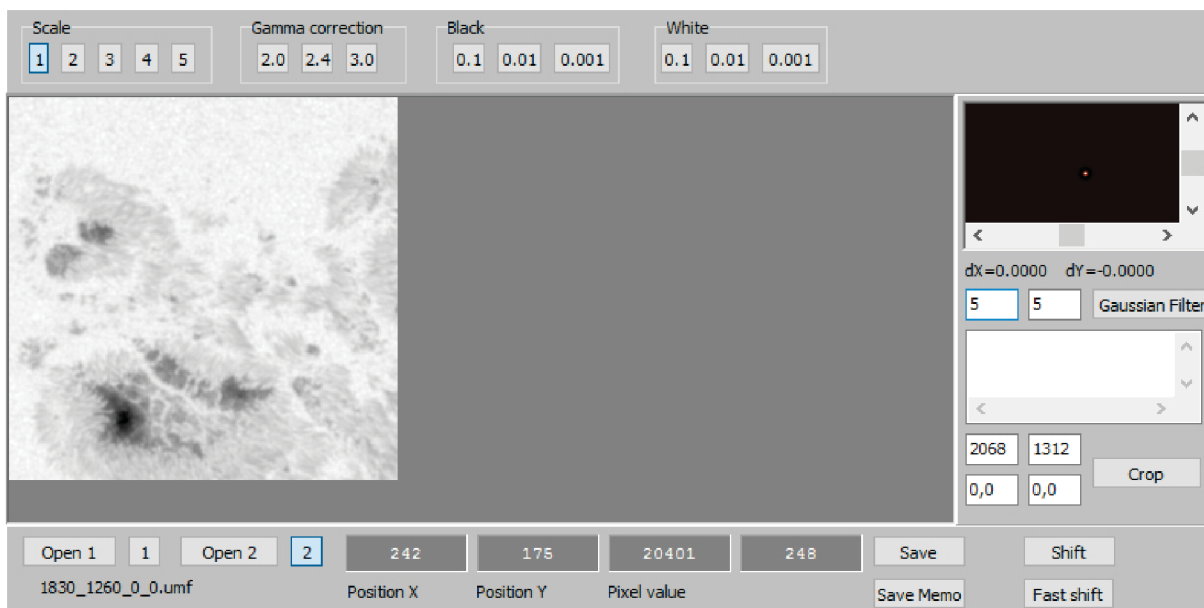


Figure 4.1: Control panel of the program

In the program there are included user-friendly elements as for example possibility to change scale or gamma correction of displayed image. User can crop and save part of image, compute shift vector of two images etc. (see Figure 4.1).

The cropping procedure **Crop** includes four Edit Boxes. Two of them for choosing the coordinates of the top left vertex of the cropped image and two remaining for choosing which shift we want to apply. If we want to crop unshifted image, it's possible to write zeros there. The exact position x, y could be found out below the image by moving cursor over it. This procedure includes bilinear interpolation. There's also save button for saving your new image to specific file.

Shift button launches procedure called **FindImgTranslation** and **DisplayPhaseCorr-Result**. The first procedure computes the shift vector, which is written up above Gaussian filter button. The second one shows us the result of phase correlation, it means that it displays the image of Dirac distribution. The final "point" will be always at the centre of top right image window (scroll-box moves with this point). Further we can use Gaussian filter button, which changes the λ_1 and λ_2 in Gaussian low-pass high-pass weight function. The shift vector, selected parameters and names of the images are written to a Memo Box. We can save these information to a text file by using Save Memo button. These method is good for finding a few possible parameters, but it's not usable with our huge number of images.

Due to the fact mentioned above, there is button called Fast shift. This button launches procedure, which computes shift vectors of all images, deviations in x, y from real shift and also maximum deviations in x, y . It is all written to a text file for later usage.

Chapter 5

Parameter Optimization

It was mentioned in Chapter 4 that we work with the set of 10 000 images. The source file `hmi.ic_45s.2014.10.23_15_00_45_TAI.continuum.fits` which contains image of the Sun obtained from SDO is downloaded from webpage of NASA, see [7]. Further we cropped out segment of size 256×256 pixels (see displayed image on left part of Figure 4.1), which we consider to be our master image. Then we cropped out sequence of new images from the source one, but now they are gradually shifted. We decided to do a percent steps, it means that each next image is shifted by 0.01 pixel up to 0.99 pixel in axis x and in the same way in axis y . At the end we had all combinations of shifts in area of one pixel.

5.1 Chosen constants and methods

Our cropped square segment has not got black edges so we need to apply Hanning rectangular window function for removing the information there. From previous studies we know that the best choice for parameter σ in the window function g_{HR} is 0.5, it means that the weight function is equal to 1 on 50 % of image.

It's possible to do phase correlation only on part of image, which is called "ROI" (Range Of Interest), it would be used, if we did not crop out the segment. In our case the ROI is identical with used image, so its width and height are 256 pixels.

The result from phase correlation is displayed as a point on black background (see Figure 5.1). We work with sub-pixel precision, such that we find maximum pixel value of this point, further we take this pixel and we will find the geometric moments of it with ε equals to 6.

5.2 Proper optimization

At the beginning of testing program we tried different λ_1 and λ_2 on few images for finding a group of parameters for next optimization. On Figure 5.1 we can see how does it work. For small λ_1 we will obtain small peak, it means that we remove only little bit of the highest frequencies and our maximum peak is steep. On the contrary, if we use big λ_1 , we will get bigger peak, it means that we remove the highest frequencies and our peak is more rounded. The parameter λ_2 changes information in the lowest frequencies so we can't see any differences in the displayed result.

For our next research we chose $\lambda_1 = \{4, 5, 6\}$ and $\lambda_2 = \{11, 12, 13, 14\}$. Thanks to

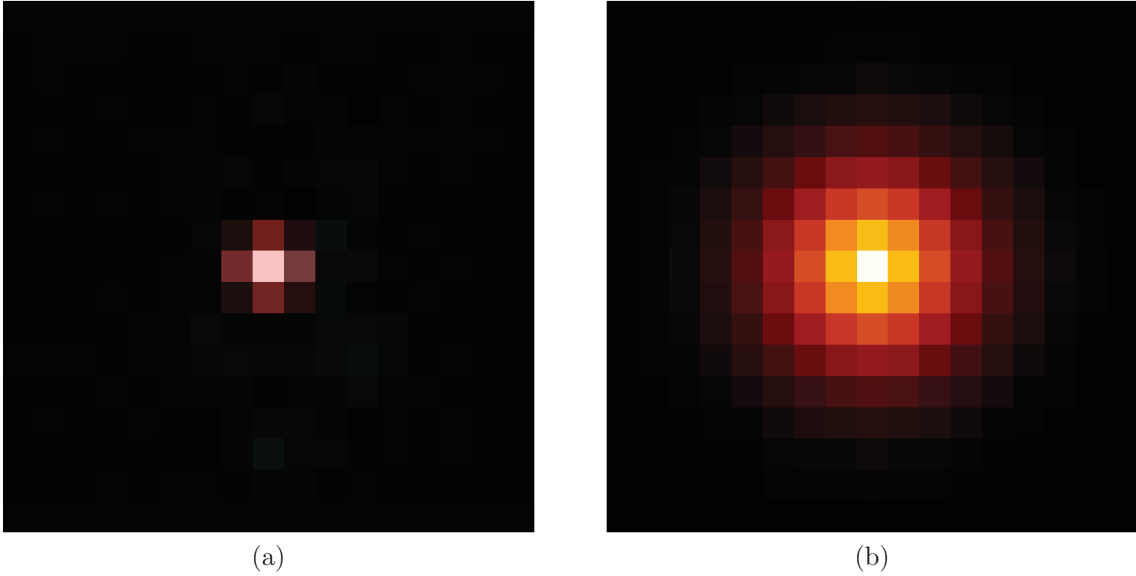


Figure 5.1: Displayed result from phase correlation after multiplication by Gaussian low-pass high-pass weight function. Used parameters $\lambda_1 = 3$ and $\lambda_2 = 13$ for image a) and $\lambda_1 = 7$ and $\lambda_2 = 13$ for image b).

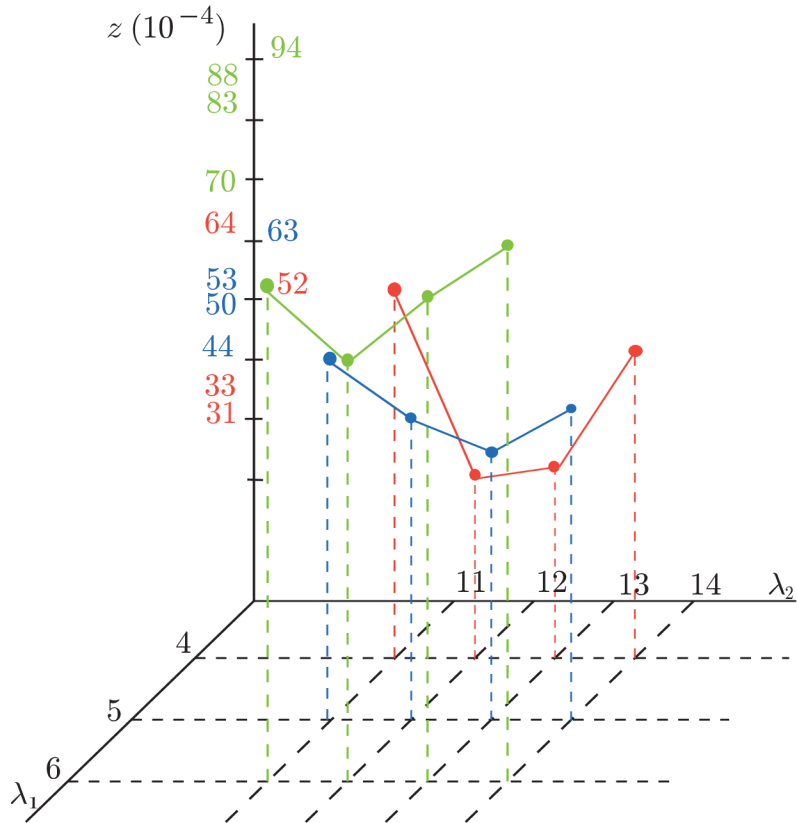


Figure 5.2: Graph of usable parameters and maximal deviations

these parameters, we can get shifts, which are identical with real shift up to thousandths. We did combinations of all these parameters and then we applied them to all images. Further we went through text files (see attachment on CD) created by this program

and we found the maximal deviations from real shifts. Then we put them to the graph (see Figure 5.2) from where we can see many information. The axis x matches to λ_1 , the axis y matches to λ_2 and the axis z equals to maximal deviations multiplied by 10^{-4} . The combinations with $\lambda_1 = 6$ are inapplicable, due to big deviations, for example the deviation for combination of $\{\lambda_1, \lambda_2\} = \{6, 14\}$ equals to 0.0094 and it's indispensable error. The combinations with $\lambda_1 = 5$ are better then the previous one, we can say that it's stationary parameter, but still we can get more exact shifts. The combinations with $\lambda_1 = 4$ are less stable then the previous one, but as we can see from graph the combination of $\{4, 12\}$ has the minimal deviation, which equals to 0.0031. Thus my chosen optimal parameters are $\lambda_1 = 4$ and $\lambda_2 = 12$.

Chapter 6

Conclusion

The goal of this thesis was to find optimal parameters of low-pass high-pass weight function (see Definition 3.6) and to make a program for computing shift vector with sub-pixel precision (see Chapter 4). For optimization we used pack of images with known shifts.

In Chapter 2 we summarised theory about phase correlation. The most important parts are definitions of Fourier transform (see Definition 2.6), convolution (see Definition 2.15), normalized cross-power spectrum (see Definition 2.19) and of course the definition of phase-correlation function (see Definition 2.22).

The Chapter 3 talks about image registration, mainly about the problems of working with real images, like presence of additive and multiple noise, dust particles and diffuse light. There is written how to abolish them also, for example by window function, which deals with big differences in image edges (see Definition 3.3). Further we wrote there about sub-pixel precision registration.

The Chapter 5 is the major part of this thesis, it is about the proper optimization. We mentioned there which constants have been used and why. We described the process of optimization and at the end we described the best parameters for sub-pixel registration as well as rationalization.

The current accuracy surpassed our expectations. We awaited that the shift vector will be precise only on hundredths, but as we can see in Figure 5.2, we are working with thousandths there. We are not in need of it, but if we wanted, we would optimize used constants (see Section 5.1) and maybe we will get even more precise shift vectors.

Bibliography

- [1] DRUCKMÜLLEROVÁ, Hana. Phase-correlation based image registration. Brno, 2010. Diplomová práce, Fakulta strojního inženýrství Vysoké učení technické v Brně.
- [2] FOLLAND, Gerald Budge. Fourier analysis and its applications. Providence, R.I.: American Mathematical Society, 2009. Sally series (Providence, R.I.), 4. ISBN 0821847902.
- [3] FRANČŮ, Jan. Parciální diferenciální rovnice. 4., dopl. vyd. Brno: Akademické nakladatelství CERM, 2011. ISBN 9788021443990.
- [4] GOSHTASBY, Ardeshir. Image registration: principles, tools and methods. London: Springer, c2012. Advances in computer vision and pattern recognition. ISBN 144712457X.
- [5] HRUŠKA, Tomáš. Pascal pro začátečníky. Praha: SNTL - Nakladatelství technické literatury, 1989. ISBN 8003003458.
- [6] KATSAGGELOS, Aggelos K. Phase correlation. In: Coursera [online]. Fundamentals of Digital Image and Video Processing: Northwestern University [cit. 2017-04-29]. Available on: <https://www.coursera.org/learn/digital/lecture/a60Ui/phase-correlation>
- [7] The Virtual Solar Observatory. The Virtual Solar Observatory [online]. NASA Goddard Space Flight Center: Solar Data Analysis Center, c2005-2017 [cit. 2017-03-27]. Available on: <http://sdac.virtualsolar.org/cgi/search>.

Used symbols

\mathbb{N}	the set of natural numbers
\mathbb{R}	the set of real numbers
\mathbb{R}^+	the set of positive real numbers, i.e. $(0, \infty)$
\mathbb{R}_0^+	the set of positive real numbers plus zero, i.e. $\langle 0, \infty$
\mathbb{C}	the set of complex numbers
$\Re F(\xi, \eta)$	the real part of Fourier spectrum
$\Im F(\xi, \eta)$	the imaginary part of Fourier spectrum
f^*	the complex conjugate of $f \in \mathbb{C}$
$f(x, y), f_1(x, y), f_2(x, y)$	functions of $\mathcal{L}(\mathbb{R}^2)$, see Definition 2.2
$F(x, y), F_1(x, y), F_2(x, y)$	the Fourier spectra of functions $f(x, y), f_1(x, y), f_2(x, y)$, see Definition 2.6
$A(\xi, \eta), A_1(\xi, \eta), A_2(\xi, \eta)$	the amplitude spectra of functions $f(x, y), f_1(x, y), f_2(x, y)$, see Definition 2.9
$\Phi(\xi, \eta), \Phi_1(\xi, \eta), \Phi_2(\xi, \eta)$	the phase spectra of functions $f(x, y), f_1(x, y), f_2(x, y)$, see Definition 2.9
$f_1(x, y) * f_2(x, y)$	the convolution of functions f_1 and f_2
$[a]$	the integer part of real number a

Attachment

CD with text files and program in Delphi XE6.

- shift-parameter-4-11.txt
- shift parameter-4-12.txt
- shift-parameter-4-13.txt
- shift-parameter-4-14.txt
- shift-parameter-5-11.txt
- shift-parameter-5-12.txt
- shift-parameter-5-13.txt
- shift-parameter-5-14.txt
- shift-parameter-6-11.txt
- shift-parameter-6-12.txt
- shift-parameter-6-13.txt
- shift-parameter-6-14.txt